

# Free Energy Barrier for Electric Field Driven Polymer Entry into Nanoscale Channels

Narges Nikoofard<sup>1</sup> and Hossein Fazli<sup>1,2,\*</sup>

<sup>1</sup>*Department of Physics, Institute for Advanced Studies in Basic Sciences (IASBS), Zanjan 45137-66731, Iran*

<sup>2</sup>*Department of Biological Sciences, Institute for Advanced Studies in Basic Sciences (IASBS), Zanjan 45137-66731, Iran*

(Dated: June 4, 2022)

Free energy barrier for entry of a charged polymer into a nanoscale channel by a driving electric field is studied theoretically and using molecular dynamics simulations. Dependence of the barrier height on the polymer length, the driving field strength, and the channel entrance geometry is investigated. Squeezing effect of the electric field on the polymer before its entry to the channel is taken into account. It is shown that lateral confinement of the polymer prior to its entry changes the polymer length dependence of the barrier height noticeably. Our theory and simulation results are in good agreement and reasonably describe related experimental data.

PACS numbers: 87.15.A-, 36.20.Ey, 87.15.H-

Interaction of polymer chains with nanoscale channels is a phenomenon of rich basic science and numerous potential applications [1–7]. Better understanding of related biological processes, analyzing biopolymers like DNA [2], investigating the existing theories on static and dynamic properties of confined polymers [3], and separation of polymers of different lengths [4, 5] are sample advantages of the experiments in which polymers are forced to interact with nanochannels. Also, this phenomenon provides possibility of observation and direct study of protein-nucleic acid interactions [6] and nucleic acids secondary structures [7]. A polymer entering into a narrow channel experiences an entropic barrier due to the reduction of its conformations and an external force should be applied to overcome this barrier. A voltage difference in the case of charged polymers like DNA [8], or flow injection may provide the driving force [9, 10].

The entry process of a charged polymer into a nanochannel in a wall under a voltage difference can be divided into two stages [11]. First, the polymer comes to the channel vicinity by a pure or electrically biased diffusion and one of its ends finds the channel entrance. Then, if the driving field overcomes the entropic barrier, the polymer enters the channel. Calculation of the barrier height as a function of the system parameters such as the driving field strength, the channel geometry, and properties of the polymer is of great importance for numerous related experiments. Polymer translocation through nanochannels and polymer escape from entropic traps which recently has been used as a polymer separation method [4, 5] are examples of such experiments. Despite extensive experimental and theoretical studies of driven polymer threading into nanoscale channels and numerous suggestions for enhancing the polymer capture rate [11–13, 17], the entry barrier height and its dependence on the system variables is less investigated.

In this paper, we calculate free energy barrier experienced by a flexible charged polymer entering into a nanochannel under an applied electric field theoretically and using coarse grained molecular dynamics (MD) sim-

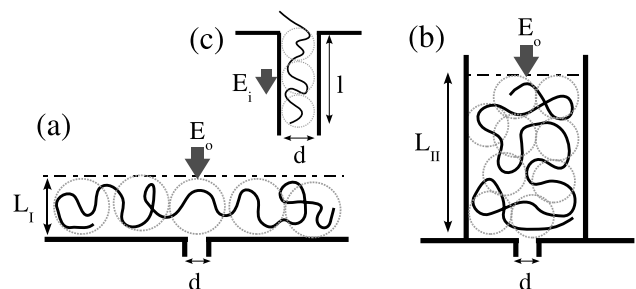


FIG. 1: Schematic of a polymer under the electric field of strength  $E_o$  behind a channel of diameter  $d$  in a wall. (a) The polymer can be viewed as a 2D chain of blobs of size  $L_I$ . (b) A polymer which is also confined laterally by a cylinder of diameter  $D$ . The polymer can be considered as a chain of blobs closely packed inside a cylinder of height  $L_{II}$ . (c) A segment of the polymer entered to the channel inside which the electric field is of strength  $E_i$ .

ulations. We obtain dependence of the barrier height on the polymer length and the driving field strength for two different geometries of the channel entrance. The external driving field could have squeezing effect on the polymer before its entry to the channel and affect its static and dynamic behaviors. Our study shows that this squeezing effect and lateral confinement of the polymer prior to the channel entry noticeably affect the dependence of the barrier height on the polymer length and the field strength. Our theoretical and MD simulation results support each other and are in reasonable agreement with some related experimental data.

To obtain free energy barrier for two channel entrance geometries shown in Fig. 1, we calculate the polymer free energy before its entry to the channel and after entering a fraction of its monomers. We assume that electric fields inside and outside of the channel are uniform and their strength may be different. As case I, consider the polymer which contains  $N$  charged monomers of diameter  $b$  and charge  $q$ , pushed to a wall by the electric field of strength  $E_o$  (see Fig. 1 (a)). We assume that there is no



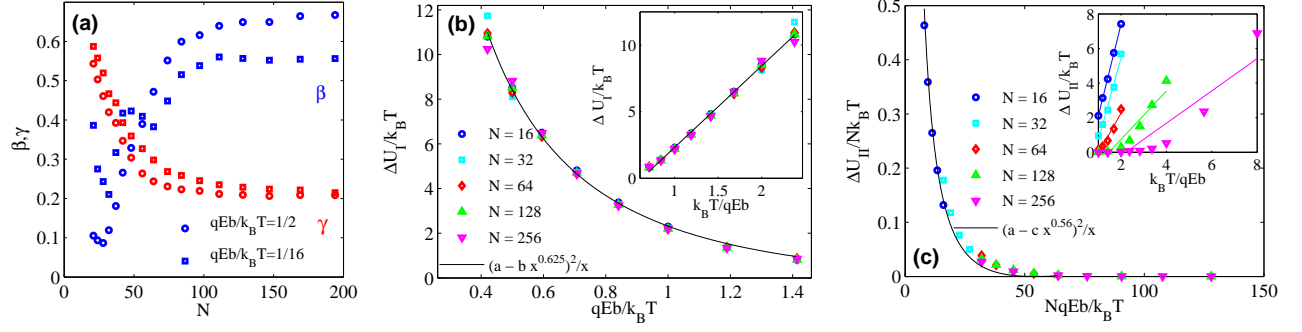


FIG. 2: (color online) (a)  $\beta$  in  $L \propto N^\beta$  and  $\gamma$  in  $R_{\parallel} L^{\frac{1}{4}} \propto N^\gamma$  versus the polymer length. With increasing  $N$  crossover from values corresponding to case *I* to those of case *II* can be seen. (b),(c) Simulation results for polymer entry barrier and fitted functions of the theory for cases *I* and *II*. Coefficients  $a=3.02$ ,  $b=1.50$  and  $c=0.32$  are fitting parameters. Considering scaled axis of these figures, agreement between simulation and theory can be seen. Insets: entry barriers versus  $E^{-1}$  and fitted lines.

electrostatic interaction between monomers (corresponding to high salt concentration) and that the monomers only interact with the electric field. The polymer decreases its electric energy by spreading on the wall in price of losing a part of its entropy. The polymer layer thickness,  $L_I$ , can be determined by balancing entropic and electric energies. In this layer, the polymer can be viewed as a 2D chain of blobs of size  $L_I$ , where the number of monomers in each blob is  $g_I \sim (\frac{L_I}{b})^{\frac{1}{\nu}}$  and  $\nu$  is the Flory exponent. Entropic energy of the polymer is  $k_B T$  per blob,  $F_{ent} \sim k_B T N \left(\frac{b}{L_I}\right)^{\frac{1}{\nu}}$ . For case *II*, consider a similar polymer which is also confined from sides by a cylinder of diameter  $D$  (see Fig. 1 (b)). Because of simultaneous confining effects of the electric field and the cylinder, this is similar to a polymer in a closed space which its blobs are closely packed. The number of monomers in each blob is given by  $g_{II} \sim \left(\frac{\Omega}{Nb^3}\right)^{\frac{1}{3\nu-1}}$ , where  $\Omega \sim L_{II} D^2$  is the confinement volume. The entropic energy of the polymer in this case is  $F_{ent} \sim k_B T \left(\frac{N^{3\nu} b^3}{\Omega}\right)^{\frac{1}{3\nu-1}}$  [9].

Electric energy of the polymer layer,  $F_{elc}$ , in both of these cases with its zero taken on the wall is  $\sim NqE_o L_m$  ( $m = I, II$ ). The equilibrium layer thickness can be obtained by minimizing total free energy  $F = F_{ent} + F_{elc}$  with respect to  $L_m$ :

$$L_I \sim b \left(\frac{qE_o b}{k_B T}\right)^{\frac{-\nu}{1+\nu}}, L_{II} \sim b \left(\frac{qE_o b}{k_B T}\right)^{\frac{1-3\nu}{3\nu}} \left(\frac{Nb^2}{D^2}\right)^{\frac{1}{3\nu}}. \quad (1)$$

Number of monomers per blob in the two cases are

$$g_I \sim \left(\frac{qE_o b}{k_B T}\right)^{\frac{-1}{1+\nu}}, g_{II} \sim \left(\frac{qE_o b}{k_B T} \frac{Nb^2}{D^2}\right)^{\frac{-1}{3\nu}}. \quad (2)$$

Free energy per monomer behind the channel is  $\sim \frac{k_B T}{g_m}$ .

Consider a polymer in each of the two cases that is going to enter a channel of diameter  $d$  on the wall. Entropic energy of each monomer after entry into the

channel is  $\sim \frac{k_B T}{g_{in}}$ , in which,  $g_{in} = \left(\frac{d}{b}\right)^{1/\nu}$  is the number of monomers per blob inside the channel. Electric energy change of  $n$  monomers after entering to the channel is  $\sim -nqE_i l$ , in which  $E_i$  is the electric field strength inside the channel and  $l = \frac{n}{g_{in}} d = n \left(\frac{b}{d}\right)^{1/\nu} d$  (see Fig. 1 (c)). Accordingly, total free energy change of the polymer after entry of  $n$  monomers is  $\Delta F_m \sim k_B T \left(\left(\frac{b}{d}\right)^{\frac{1}{\nu}} - \frac{1}{g_m}\right) n - n^2 qE_i \left(\frac{b}{d}\right)^{1/\nu} d$ . Free energy barrier height for the polymer entry,  $\Delta U_m$ , is the maximum of  $\Delta F_m$  with respect to  $n$  and is given by

$$\frac{\Delta U_m}{k_B T} \sim \left(\left(\frac{b}{d}\right)^{\frac{1}{\nu}} - \frac{1}{g_m}\right)^2 \frac{k_B T}{qE_i d} \left(\frac{d}{b}\right)^{1/\nu}. \quad (3)$$

In simulations for checking our theory, we model the polymer by  $N$  spherical monomers of diameter  $\sigma$  connected by FENE potential. Shifted and truncated Lennard-Jones potential is used to model monomer-monomer and monomer-wall excluded volume interactions and it is assumed that  $E_o = E_i = E$ . All our simulations are performed with ESPResSo [14] using Langevin thermostat to keep the temperature fixed.

To check our theoretical results on static behavior of the polymer before its entry to the channel, we measure some variables in our simulations by keeping the channel closed and letting the polymer to fluctuate behind it. Lateral gyration radius of a polymer confined between two planes of spacing  $L$  is  $R_{\parallel} \sim N^{\frac{2}{3}} b \left(\frac{b}{L}\right)^{\frac{1}{4}}$  [9]. For a fixed diameter of the confining cylinder,  $D = 12\sigma$ , exponents  $\beta$  and  $\gamma$  in relations  $L \propto N^\beta$  and  $R_{\parallel} L^{\frac{1}{4}} \propto N^\gamma$  are obtained via local slopes of the log-log plots of  $L$  and  $R_{\parallel} L^{\frac{1}{4}}$  versus  $N$ . Results for two different field strengths are shown in Fig. 2 (a). For a fixed value of  $D$ , short and long polymers correspond to cases *I* and *II*, respectively. With increasing  $N$ , crossover from case *I* with expected exponents  $\beta_I = 0$  and  $\gamma_I = 0.75$  to case *II* with  $\beta_{II} = \frac{1}{3\nu} \simeq 0.6$  and  $\gamma_{II} = \frac{1}{12\nu} \simeq 0.14$  can be seen in Fig. 2 (a). The value of  $\alpha$  in relation  $L \propto E^{-\alpha}$  is



also obtained from simulations for three different polymer lengths. For both cases *I* and *II*, it is found that  $\alpha \simeq 0.4$ , in agreement with the theory. Results on static behavior of the polymer is of importance in the subject of polymer compression by external force in nanochannels [15]. As an example and for comparison with experiment, the change in the free energy of a polymer arising from its confining in a narrow channel under an electric field can be written from case *II* of our theory as  $\frac{\Delta F}{k_B T} \sim \frac{N}{g_{II}} \propto N^{1.6}$ . This is in excellent agreement with experimental result of Ref. [16].

To check the main result of our theory, Eq. 3, we measure the barrier height for the polymer entry for each given set of  $N$  and  $E$  in both of cases *I* and *II*. We fix the end monomer of the polymer at the channel entry and leave the other monomers to equilibrate under the applied electric field. Then we release the polymer end to probe whether its entry is successful or no. We obtain  $-\frac{\Delta U}{k_B T}$  as the logarithm of successful entry probability (fraction of at least  $10^3$  simulations in which the polymer entry is successful). Results for polymers of different lengths at different values of the electric field strength are shown in Fig. 3 (b) and (c). As it can be seen, there is a very good agreement between our theory and simulation results in both of the two cases. In the insets of Fig. 2 (b) and (c), deviation of  $\Delta U$  versus  $E^{-1}$  from linear form in large intervals of  $E$  in both cases, no dependence of entry barrier on polymer length in case *I* contrary to case *II*, and decrease of entry barrier with the polymer length in case *II* can be seen. These results are different from predictions of the previous theories: linear decrease of the barrier height with the applied voltage [13] and its dependence on the polymer length even for simple pores [17]. In previous studies, dependence of the barrier height on  $N$  is attributed to the restriction of the polymer end to the channel during its entrance [18]. Because of the compression effect of the driving field which is taken into account in our work, only monomers in the first blob feel the restriction and its energy cost is independent of  $N$ .

One should note that the validity range of our theory in both cases is  $1 \leq g_m \leq N$ .  $g_m > N$  means that the electric field is too weak to has confining effect on the polymer behind the channel and cannot overcome the entropic barrier. Consistent with this description, in simulations with smaller polymers and lower electric fields, we obtained  $\alpha \simeq 0$  and  $\beta \simeq \nu$ .  $g_m < 1$  means that the polymer loses most of its entropy behind the channel and feels no entropic barrier on its entry (as simulation results also show in Fig. 2 (b) and (c)). Existence of two voltage limits, the one below which no polymer entry happens and another one above which voltage dependence of the capture time changes from exponential to linear function [12, 19] could be related to these limits.

In voltage driven polymer translocation experiments, one of the measurable quantities is the capture time,  $\tau$ ,

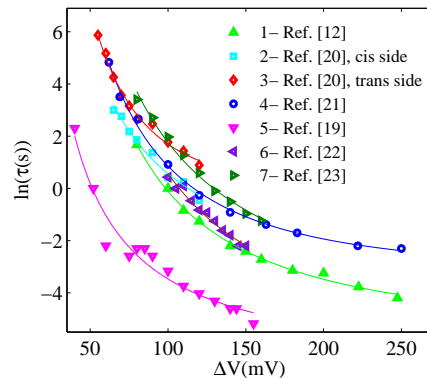


FIG. 3: (color online) Logarithm of capture time versus  $\Delta V$  extracted from referenced articles (symbols) and fitted equation of our theory, Eq. 4 (solid lines). All the data sets are from polymer translocation experiments through  $\alpha$ -hemolysin channel. As it can be seen, all data sets are followed well by the suggested function. Fit parameters are shown in Table I.

TABLE I: Parameters  $\zeta$ ,  $\eta$ , and  $\lambda$  obtained from fitting of Eq. 4 to seven data sets shown in Fig. 3.

	Experimental data	$\zeta$	$\eta$	$\lambda$
1	ssDNA, cis side (Ref. [12])	-5.42	3.14	0.60
2	ssDNA, cis side (Ref. [20])	-4.33	2.38	0
3	ssDNA, trans side (Ref. [20])	0.27	3.22	1.77
4	ssDNA, cis side (Ref. [21])	-3.01	3.11	0.90
5	DS, cis side (Ref. [19])	-7.09	2.35	0.01
6	DS, trans side (Ref. [22])	-6.13	3.85	0.51
7	PSS, cis side (Ref. [23])	-6.01	2.83	0

at different voltage differences,  $\Delta V$  [11, 12, 19–23]. The average capture time can be written from Van’t Hoff-Arrhenius law as  $\tau = \tau_0 \exp\left(\frac{\Delta U}{k_B T}\right)$  [20], in which  $\Delta U$  is the free energy barrier height.  $\tau_0^{-1}$  is the frequency of polymer fluctuations behind the channel when entry of folded polymer is possible [24] or frequency of the polymer ends reaching to the channel entrance when entry of folded polymer is not possible. From Van’t Hoff-Arrhenius law and eq. 3 of the theory, and considering that  $1/(1+\nu) \simeq 1/3\nu \simeq 0.6$ , the equation

$$\ln \tau = \zeta + \left( \eta - \lambda \left( \frac{qE_i b}{k_B T} \right)^{0.6} \right)^2 \frac{k_B T}{qE_i b} \quad (4)$$

can be used for fitting to experimental data by  $\zeta$ ,  $\eta$ , and  $\lambda$  as the fit parameters, regardless of the similarity of the channel entrance geometry to case *I* or *II* of the theory. In equation 4, we have assumed  $E_i \simeq \frac{\Delta V}{\ell}$  and  $E_o = \delta E_i$ , where  $\ell$  is the channel length and  $\delta < 1$  (there is no satisfactory knowledge about values and spatial functionality of  $E_i$  and  $E_o$ ). Also,  $b$  and  $q$  are obtained by coarse-graining the polymer such that the size of effective spher-



ical monomers is equal to the polymer diameter. For example, for translocation of single stranded DNA (ssDNA) through  $\alpha$ -hemolysin channel at the room temperature, we use  $\ell = 10nm$ ,  $b = 1nm$ , and  $q = 3e$  ( $e$  is the electron charge), which results in  $\frac{qE_b}{k_B T} \simeq 0.01\Delta V(mV)$ . It should be noted that from the Van't Hoff-Arrhenius law  $\zeta = \ln \tau_0$  and from Eqs. 2 and 3,  $\eta \sim \left(\frac{d}{b}\right)^{\frac{1}{2}-\frac{1}{2\nu}}$  for both of the two cases,  $\lambda \sim \left(\frac{d}{b}\right)^{\frac{1}{2}+\frac{1}{2\nu}} \delta^{0.6}$  for case *I* and  $\lambda \sim \left(\frac{d}{b}\right)^{\frac{1}{2}+\frac{1}{2\nu}} \delta^{0.6} \left(\frac{Nb^2}{D^2}\right)^{0.6}$  for case *II*.

In Fig. 3,  $\ln \tau$  versus  $\Delta V$  reported for translocation of three flexible polymers, ssDNA, dextran sulfate (DS), and poly(styrenesulfonic acid) (PSS), from cis and trans sides of  $\alpha$ -hemolysin channel and fitted function of Eq. 4 are shown. The values of fitting parameters are shown in Table I.  $\zeta$  in Eq. 4 depends only on  $\tau_0$  which is out of interest here.  $\eta$  depends on the ratio of the channel diameter to the monomer size and as all the seven data sets shown in Fig. 3 are for experiments with the same channel,  $\alpha$ -hemolysin, similar values of  $\eta$  is reasonable. The most important parameter which is a measure of the squeezing effect of the electric field on the polymer before its entry to the channel is  $\lambda$ . For data sets 2, 5 and 7, where polymer is added to the cis side and applied voltages are relatively low (up to 160 mV),  $\lambda$  is negligible. This is because of the weak electric fields which results in small squeezing effects. Nonzero value of  $\lambda$  with similar applied voltages for the trans side (data sets 3 and 6), could be because of the smaller diameter of the channel in this side which causes the electric field in the vicinity of the channel entrance to be stronger and the parameter  $\delta$  to be larger [25]. It should be noted that according to ref. [12], compression of the polymer inside the cis side vestibule of  $\alpha$ -hemolysin channel happens very rarely. So entry of the polymer from both the cis and trans sides is similar to case *I* of the theory (and not the case *II*). For the cis side, data sets 1 and 4, applied voltages are higher (up to 280 mV) which makes the squeezing effect more considerable and the value of  $\lambda$  nonzero.

In summary, free energy barrier height for electric field driven polymer entry into channels of two different entrance geometries has been calculated theoretically and by MD simulations. The barrier height dependence on the electric field strength and the polymer length, the effect of lateral confinement of the polymer before its entry to the channel on these dependencies and relevance of results with experiment have been discussed.

We are grateful to Mohammad R. Kolahchi for useful comments.

---

\* Electronic address: fazli@iasbs.ac.ir

[1] A. Meller, J. Phys. Condens. Matter **15**, R581 (2003); C. Dekker, Nature Nanotech. **2**, 209 (2007); H. Craighead,

- Nature **442**, 387 (2006).  
 [2] D. Branton *et al*, Nature Biotech. **26**, 1146 (2008); M. Zwolak, and M. Di Ventra, Rev. Mod. Phys. **80**, 141 (2008).  
 [3] L. Movileanu, and H. Bayley, Proc. Natl. Acad. Sci. U.S.A. **98**, 10137 (2001); S. Howorka *et al*, J. Am. Chem. Soc. **122**, 2411 (2000); J. O. Tegenfeldt *et al*, Proc. Natl. Acad. Sci. U.S.A. **101**, 10979 (2004); W. Reisner *et al*, Phys. Rev. Lett. **94**, 196101 (2005); S. van Dorp *et al*, Nature Phys. **5**, 347(2009); W. Reisner *et al*, Phys. Rev. Lett. **99**, 058302 (2007); C. Zhang, P. G. Shao, J. A. van Kan, and J. R. C. van der Maarel, Proc. Natl. Acad. Sci. U.S.A. **106**, 16651 (2009); T. Uemura *et al*, Nature Commun. **1**, 83 (2010).  
 [4] J. Han, S. W. Turner, and H. G. Craighead, Phys. Rev. Lett. **83**, 1688 (1999).  
 [5] J. T. Mannion, C. H. Reccius, J. D. Cross, and H. G. Craighead, Biophys. J. **90**, 4538 (2006); K. D. Dorfman, Rev. Mod. Phys. **82**, 2903 (2010); R. B. Schoch, J. Han, and P. Renaud, Rev. Mod. Phys. **80**, 839 (2008).  
 [6] B. Hornblower *et al*, Nature Methods **4**, 315 (2007); S. W. Kowalczyk, A. R. Hall, and C. Dekker, Nano Lett. **10**, 324 (2010); J. Lin, A. Kolomeisky, and A. Meller, Phys. Rev. Lett. **104**, 158101 (2010).  
 [7] A. F. Sauer-Budge, J. A. Nyamwanda, D. K. Lubensky, and D. Branton, Phys. Rev. Lett. **90**, 238101 (2003); R. Bundschuh, and U. Gerland, Phys. Rev. Lett. **95**, 208104 (2005).  
 [8] J. J. Kasianowicz, E. Brandin, D. Branton, and D. Deamer, Proc. Natl. Acad. Sci. U.S.A. **93**, 13770 (1996).  
 [9] T. Sakaue, and E. Raphael, Macromolecules **39**, 2621 (2006).  
 [10] D. Stein, F. H. J. van der Heyden, W. J. A. Koopmans, and C. Dekker, Proc. Natl. Acad. Sci. U.S.A. **103**, 15853 (2006).  
 [11] M. Wanunu *et al*, Nature Nanotech. **5**, 160 (2010).  
 [12] G. Maglia, M. R. Restrepo, E. Mikhailova, and H. Bayley, Proc. Natl. Acad. Sci. U.S.A. **105**, 19720 (2008).  
 [13] T. Chou, J. Chem. Phys. **131**, 034703 (2009); A. Y. Grosberg, Y. Rabin, J. Chem. Phys. **133**, 165102 (2010).  
 [14] H. J. Limbach, A. Arnold, B. A. Mann, C. Holm, Comp. Phys. Communications **174**, 704 (2006).  
 [15] C. H. Reccius, J. T. Mannion, J. D. Cross, and H. G. Craighead, Phys. Rev. Lett. **95**, 268101 (2005); S. Jun, D. Thirumalai, and B.-Y. Ha, Phys. Rev. Lett. **101**, 138101 (2008).  
 [16] T. K. Rostovtseva, E. M. Nestorovich, and S. M. Bezrukov, Biophys. J. **82**, 160 (2002).  
 [17] M. Muthukumar, J. Chem. Phys. **132**, 195101 (2010).  
 [18] J. Chuang, Y. Kantor, M. Kardar, Phys. Rev. E, **65**, 011802 (2001); R. Kumar, M. Muthukumar, J. Chem. Phys. **131**, 194903 (2009).  
 [19] L. Brun *et al*, Phys. Rev. Lett. **100**, 158302 (2008).  
 [20] S. E. Henrickson, M. Misakian, B. Robertson, and J. J. Kasianowicz, Phys. Rev. Lett. **85**, 3057 (2000).  
 [21] A. Meller, and D. Branton, Electrophoresis **23**, 2583 (2002).  
 [22] G. Gibrat *et al*, J. Phys. Chem. B, **112**, 14687 (2008).  
 [23] Q. Chen *et al*, Macromolecules **43**, 10594 (2010).  
 [24] P.J. Park, and W. Sung, J. Chem. Phys. **111**, 5259 (1999).  
 [25] S. Howorka, and H. Bayley, Biophys. J. **83**, 3202 (2002).